

1 Backdraft Experiments and Large Eddy Simulations in a Scaled Compartment

2 Marcos Vanella^{a*}, Ryan Falkenstein-Smith^a, and Thomas Cleary^a

3 ^aNational Institute of Standards and Technology, Gaithersburg, USA

4 marcos.vanella@nist.gov

5 *Corresponding author

6 Highlights:

- Initial conditions for computer fire models are defined from an extensive dataset of backdraft experiments performed at NIST.
- Chemical composition and heat measurements from these experiments are intended to assess fire models.
- The Fire Dynamics Simulator with fast chemistry is exercised on some of these backdraft scenarios.
- For mix-controlled fast reactions, ignition model temperature threshold and ignition procedure are found to play a primary role in backdraft outcomes.

15 Abstract: An extensive set of backdraft experiments has been performed at the NIST National
16 Fire Research Laboratory. These experiments were conducted in a reduced scale compartment,
17 and are part of defining the conditions conducive to backdraft. Further, the detailed chemistry and
18 heat measurements are intended to evaluate computational fire models. In this article, we describe
19 the modeling effort employing the Fire Dynamics Simulator (FDS) in simulations involving
20 different fuels and ignition source locations mirroring a subset of the named experiments. We
21 focus on using default simulation parameters and study their effect on the backdraft outcomes. In
22 particular, the ignition model's temperature threshold and ignition procedure play a primary role
23 in developing a backdraft.

24 Keywords:

25 Backdraft Experiments; Fire Simulation; FDS; Large Eddy Simulation;

26 1. Introduction

27 Backdrafts pose a life-threatening risk to any firefighter that may encounter them. A backdraft is a
28 deflagration resulting from igniting an incoming gravity current of air mixed with a heated,
29 fuel-rich, and oxygen-depleted environment [?]. Several experimental works have identified the
30 physical mechanisms and conditions conducive to backdrafts. Fleischmann examined the thermal
31 and gas compositions within an enclosure's environment influencing the incoming gravity
32 current [?, ?]. Gottuk and others [?] estimated critical mass fractions in vitiated atmospheres,
33 resulting in backdraft using full-scale steel compartments. Wu and colleagues [?] established a
34 correlation between the likelihood of backdraft and compartment configuration by varying

35 ventilation conditions, ignition locations, and mass fluxes of gas leakage. Other works have
36 studied the probability of backdraft generated from solid fuel combustion within an
37 enclosure [?, ?, ?].

38 On the other hand, several studies have relied on computational models utilizing large eddy
39 simulation (LES), particularly the Fire Dynamics Simulator (FDS), to simulate backdraft. In
40 general, these studies use finite-rate chemistry and several-step reactions to capture deflagration
41 physics. For example, Weng, Fan, and Hasemi used LES to predict the ignition time for backdraft
42 in compartments with different opening geometries [?]. Ferraris and others implemented a
43 subgrid-scale model based on mixture fraction to define partially premixed combustion applied to
44 backdraft [?]. Park et al. used single and three-step finite rate chemistry in FDS to investigate the
45 relationship between the initial fuel mass in a compartment and the resulting backdraft [?]. Ashok
46 and Echekki used FDS to study the effect of the gravity current magnitude on backdraft
47 events [?]. Of particular interest is the work of Myilsamy et al., who used single-step fast
48 chemistry to study the fuel fraction required for backdraft in different opening geometries [?].
49 Several of these studies have established the critical elements that impact the generation of a
50 backdraft. Yet, to date, a constraint has been the limited availability of comprehensive
51 experimental datasets to compare simulation results.

52 Recently, an extensive series of 500 experiments focused on examining backdraft in a
53 reduced-scale enclosure was performed at the NIST National Fire Research Laboratory [?]. The
54 experimental series generated an extensive dataset that identifies environmental conditions
55 indicative of backdraft under various configurations, including gaseous fuel type, fire size, spark
56 location, and compartment opening configuration. The substantial range of comprehensive
57 measurements provides detailed information that can be used to evaluate computational models.
58 In this work, the wealth of experimental data produced is leveraged to assess the FDS default LES
59 combustion models for backdraft, particularly two-step mixing controlled fast reactions in
60 development for engineering applications.

61 The next section describes experiments and their use in defining initial conditions within the
62 compartment for backdraft simulation. Then, the standard FDS combustion model and the
63 backdraft model setup are given in section 3. A grid sensitivity study and comparison with
64 experiments on representative backdraft cases using methane and propane is shown in section 4,
65 and most importantly, effects of the re-ignition model and ignition procedure in deflagration
66 outcomes are presented in sections 5 and 6. Finally, some conclusions are provided in section 7.

67 **2. Experimental Method: Definition of compartment initial conditions**

68 A schematic of the 1 m by 1 m by 1.5 m reduced-scale enclosure used for all experiments is
69 provided in Figure 1. The enclosure was designed to scale, 2/5th the dimensions of an ASTM test
70 room. Experiments were initiated when a square sand burner, with a 17.8 cm side length, was
71 ignited. In these experiments, the sand burner's center was approximately 0.5 m from either side
72 wall and 1.25 m from the front opening. After the initial ignition, the fire size increased to a
73 predetermined heat release rate and was allowed to burn with the compartment door open for 60 s.

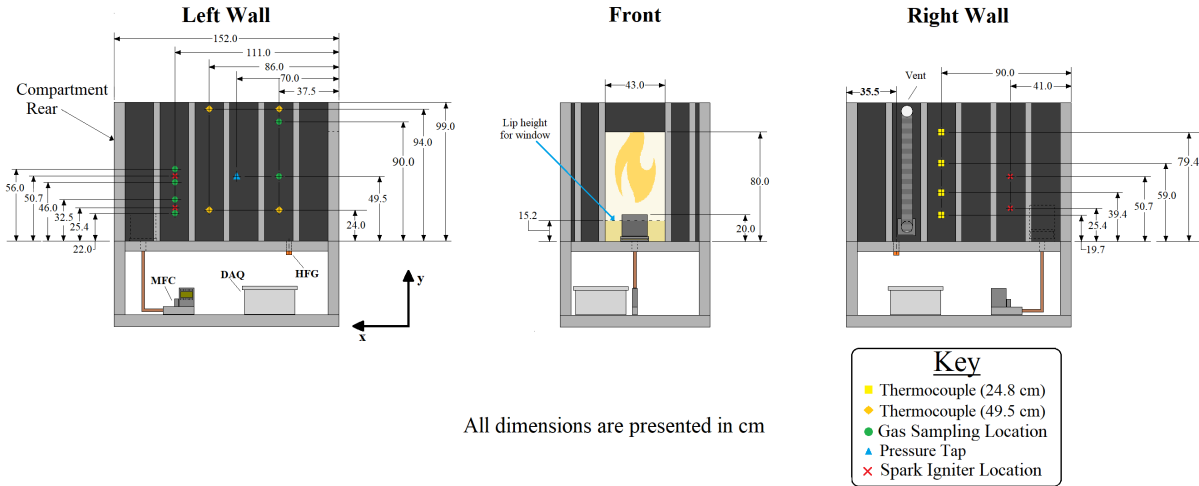


Figure 1. Schematic of the 2/5th scale compartment used in backdraft experiments

74 Afterward, the door was shut. While the doorway was closed, fuel continued to flow through the
 75 burner for a predetermined duration, and when reached, the flow was stopped. The fuel flow
 76 durations used in this work are shown in Table 1, corresponding to their respective fire sizes. The
 77 compartment remained closed for an additional 30.0 s after the fuel flow duration to allow the
 78 internal gases to form a more homogenous mixture. Once the door opened, spark ignitors were
 79 triggered, providing a continuous ignition source for the residing fuel and incoming gravity
 80 current of air.

Table 1: List of fuel flow times for each fire configuration

Fuel	Fire size (kW)	Fuel flow time [FFT] (s)
Methane	25.0 ± 1.0 kW	360, 390, 450
	37.5 ± 1.0 kW	225, 285
Propane	16.7 ± 1.0 kW	255, 270, 315
	25.0 ± 1.0 kW	210, 285

81 The locations of the spark ignitors, thermocouples, and gas sampling locations are displayed in
 82 Figure 1. The spark ignitors were positioned either 25.4 cm ('low spark') or 50.7 cm ('mid
 83 spark') from the compartment floor. Thermocouples were incorporated on both side walls of the
 84 compartment in two different configurations. The first thermocouple configuration used 49.5 cm
 85 long, 0.3175 cm diameter sheathed Type K thermocouples configured in a rectangular orientation
 86 on the left wall facing the door. The second thermocouple array included four 24.8 cm long,
 87 0.3175 cm diameter sheathed Type K thermocouples configured in a line on the right wall facing
 88 the door spaced approximately 19.9 cm apart. Gas samples were portioned and analyzed into two
 89 gas analyzers and phi meters at one of three location pairs displayed in Figure 1. The gas analyzer
 90 included one paramagnetic and two nondispersive infrared sensors to measure oxygen, carbon
 91 dioxide, and carbon monoxide, respectively. The phi meter [?, ?] provided equivalence ratio

92 measurements of the extracted gas sample. A combination of the gas analyzer and phi meter
 93 measurements was used to estimate the concentration of major species adjusted to a wet basis.
 94 Major gas species included methane/propane, oxygen, carbon dioxide, carbon monoxide, water
 95 vapor, and nitrogen. Gas and temperature measurements were monitored using a data acquisition
 96 system sampling 1.0 Hz during each experiment. Each experiment was recorded using two
 97 external cameras, with one placed nominally 5.5 m from the front and another approximately
 98 4.7 m from the side of the compartment. A detailed description of the compartment is available in
 99 Ref. [?].

100 Initial conditions for backdraft models were determined in two-compartment zones from
 101 time-averaged temperature and estimated gas concentration measurements averaged over repeated
 102 experiments with the same fuel flow duration and fire size. Zones were divided at the height of
 103 39.25 cm from the species concentration measurements observed to be fairly homogeneous.
 104 Time-averaged measurements were calculated from a 10.0 s time domain immediately before the
 105 compartment doorway opening.

106 An estimated gravity current velocity was computed using Eq. (1), which utilizes a Froude
 107 number. The Froude number was determined from the ratio of the observed velocity of the gravity
 108 current, and the root of the product of the normalized positive density difference, β , the
 109 compartment height, h (1.0 m), and the gravitational constant, g (9.81 m s^{-2}). The observed
 110 velocity of the gravity current was estimated from the video recordings of the front of the
 111 compartment that captured the time to ignition from when the door opened. The density within
 112 the compartment before the door opened, ρ , and the density of the ambient fluid within the gravity
 113 current, ρ_o , estimated to be $1.19 \text{ g/L} \pm 0.01$ from sensors outside of the compartment were used
 114 to calculate β . The gas mixture density within the compartment before the door opened was
 115 determined from the gas concentrations measured using the gas analyzer and phi meter. The
 116 average Froude number was determined to be 0.2 ± 0.05 .

$$U_{est} \approx \frac{1}{5} \sqrt{\beta h g} ; \quad \beta = \frac{\rho_o - \rho}{\rho} \quad (1)$$

117 The uncertainty of the experimental measurements was determined from a combination of the
 118 Type A and B evaluation of uncertainty. The Type A evaluation of uncertainty was estimated from
 119 the variance of the averaged measurements. The Type B evaluation of uncertainty was determined
 120 from the reported instrumentation error. The variance between the averaged measurements was
 121 determined to be the dominant contributor to the estimated uncertainty.

122 Backdraft intensity was estimated from the total heat release of the exiting flame. During each
 123 experiment, the compartment was placed under a canopy hood with a 3.0 MW calorimetry
 124 measurement system. In this instance, the total heat release was estimated using carbon dioxide
 125 generation calorimetry with a correction for carbon monoxide generation to account for unburned
 126 fuel exiting the compartment. The total heat release, THR , was calculated using Eq. 2:

$$THR = \sum_{t=0}^{\infty} \left[\dot{m}_{CO_2}(t) \left(\frac{LHV_F \text{ MW}_F}{x \text{ MW}_{CO_2}} \right) + \dot{m}_{CO}(t) \left(\frac{LHV_F \text{ MW}_F}{x \text{ MW}_{CO}} - \Delta H_{C,CO}^o \right) \right] \Delta t \quad (2)$$

127 Here, $\dot{m}_{\text{CO}_2}(t)$ and $\dot{m}_{\text{CO}}(t)$ represent the mass flow rate of CO_2 and CO measured in the duct,
 128 respectively. The number of carbon atoms and lower heating value of the parent fuel are
 129 represented by x and LHV_F , respectively. The molecular weight of the parent fuel, carbon
 130 dioxide, and carbon monoxide is denoted as MW_F , MW_{CO_2} , and MW_{CO} , respectively. The heat
 131 of combustion for carbon monoxide, $\Delta H_{\text{C},\text{CO}}^\circ$ used in Eq. 2 was 10.10 kJ/g as reported by
 132 Ref. [?]. The heat released from the combustion gases trapped in the compartment before opening
 133 the door is subtracted from the measured total heat released for a backdraft estimated from scores
 134 of experiments that did not ignite and produce a deflagration.

135 The probability of backdraft for different compartment configurations was determined from a
 136 regression fitting. The regression fitting incorporated the number of times a backdraft was
 137 observed over the total number of times the experiment was conducted under the same condition
 138 as a function of the total chemical energy within the compartment before an anticipated backdraft.
 139 Two different regression fittings for the likelihood of backdraft were calculated for different spark
 140 locations.

141 **3. Numerical Method and Model setup**

142 The Fire Dynamics Simulator (FDS) is a fire modeling software developed by the Fire Research
 143 Division of the National Institute of Standards and Technology, USA. It solves combusting,
 144 thermally buoyant flows with application to design and evaluation of fire protection systems, fire
 145 forensics studies, and general fire research, among others. Large eddy simulation based on eddy
 146 viscosity models, species transport, combustion, and radiation numerical models are at the core of
 147 this application. Of primary importance to the present work is the treatment of combustion in
 148 FDS, particularly the use of fast chemical reactions, which is essential to simulate realistic
 149 engineering problems in a cost-efficient manner. Fire generally involves non-premixed
 150 combustion, therefore, species mixing controlled reactions are treated using the Eddy Dissipation
 151 Concept (EDC) model [?]. Here, the volumetric mass of fuel consumed by the chemical
 152 combustion process is approximated as

$$\dot{m}_f''' = -\rho \frac{\min(Y_f, Y_{ox}/s)}{\tau_{mix}} \quad (3)$$

153 where ρ is the local cell density, Y_f , Y_{ox} are the corresponding fuel and oxidizer mass fractions, s
 154 is the stoichiometric ratio of the reaction, and τ_{mix} is the mixing process time scale that needs to
 155 be modeled [?]. From the volumetric mass consumption (or production) of the chemical species
 156 involved in the reaction, the heat release rate per unit volume, (HRRPUV) can be computed as

$$\dot{Q}''' = - \sum_j \dot{m}_j''' \Delta h_{f,j}^\circ \quad (4)$$

157 where \dot{m}_j''' volumetric mass rate of change of species j , and $\Delta h_{f,j}^\circ$ is its enthalpy of formation.
 158 EDC and fast kinetics dispense with the need to integrate in-time reaction evolution equations on
 159 each computational cell, which generally becomes prohibitively costly for practical engineering

problems. It also holds the unphysical assumption that any amount of fuel and oxidizer that mix will combust (so-called "mixed is burnt") regardless of their thermodynamic state. This leads to the need to define an additional scheme to specify whether the chemical components on a computational cell react. In FDS, two extinction models are present. These models follow empirical rules, based on the definition of critical flame temperature T_{CFT} [?]:

- EXTINCTION_1 : This model is based on the concept of limiting oxygen concentration [?] $X_{o_2,lim}$ which is assumed a linear function of the T_{CFT} up to a "free burn temperature threshold" T_{fb} . If the cell oxygen concentration is less than $X_{o_2,lim}$, combustion is suppressed. The default value of T_{fb} is 600 °C, consistent with experimental oxygen concentration readings in the upper layer of flashover compartments [?, ?].
- EXTINCTION_2: This model uses both fuels and oxygen concentrations in a given computational cell. If the potential heat release of a chain of reactions cannot increase the cell temperature over the T_{CFT} , combustion is suppressed, and initial values of reactants in the cell are restored.

A detailed description of these models and their implementation is given in [?].

Additionally, commonly in numerical simulations, the species composition in a computational cell is such that combustion can proceed by the extinction model, even though mean cell temperatures are low. Consequently, flames will be seen in regions where gas and air blend at nearly ambient temperature. These spurious flames are called, in practice, "ghost flames". To avoid this unphysical re-ignition, an ignition model has to be added. A simple model is used in FDS, where the cell temperature has to be higher than a threshold value T_{TH} for the reaction to be allowed to proceed. The value of T_{TH} is, in general, dependent on the type of problem and grid resolution, with the fuel auto-ignition temperature (AIT) [?] being technically correct for highly resolved direct numerical simulations (DNS). The SFPE Handbook values for different fuels are used as default T_{TH} in FDS.

A computational model was created to simulate with FDS the backdraft experiments given a representative set of species concentration and temperature initial conditions. FDS6.7.9-1409 was compiled from source using the Intel® OneAPI toolchain and used in this work. The Smokeview [?] render of the domain, compartment and ignition/data collection devices can be seen in Figure 2a. In all computations, the domain is of size 4.56 m x 2.22 m x 4.84 m in the x, y, z directions, deemed appropriate to capture the combustion region inside and outside the compartment correctly. The domain is divided into 48 meshes. Computations were done using FDS MPI parallel processing capability. The two-step simple chemistry model for fast reactions [?] was employed to accommodate the different species defined from the experiment (fuel, oxygen, carbon monoxide, carbon dioxide, water vapor, and soot). Default parameters for the chemistry model were used, and soot yields were set to 0.001 kg/kg for methane and 0.024 kg/kg for propane [?]. Different grid sizes were evaluated for the range of cases defined by experimental initial conditions: coarse grid $\Delta x = 5.7$ cm, medium grid $\Delta x = 2.8$ cm, and fine grid $\Delta x = 1.4$ cm. Cells were approximately cubed and kept constant in the domain. Also, for two representative backdraft cases shown below, a very fine grid with $\Delta x = 0.7$ cm was used to

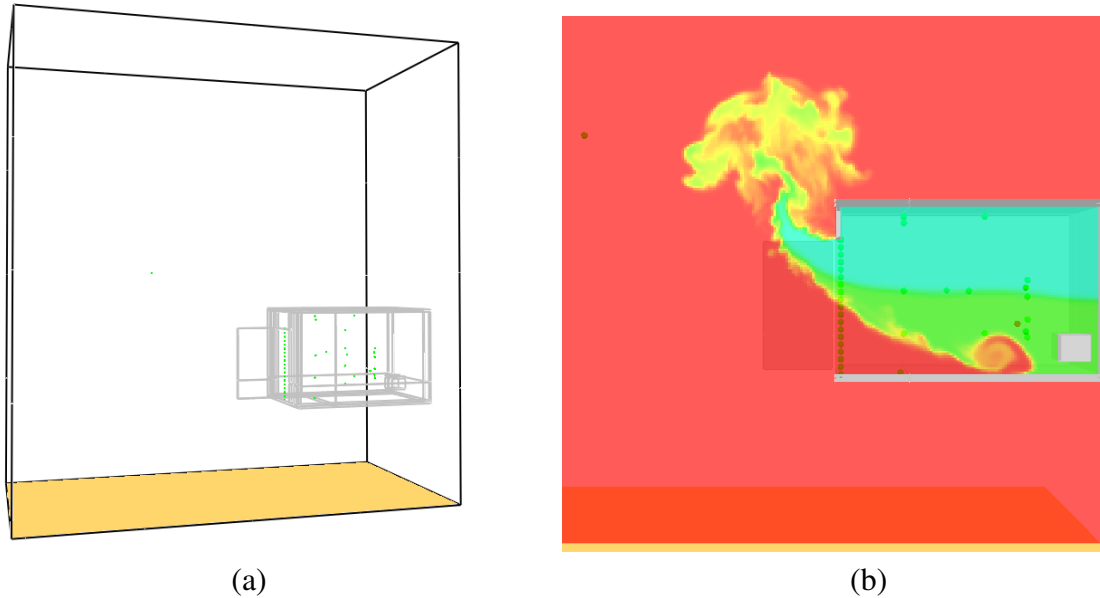


Figure 2. Backdraft computational model : (a) Domain and compartment geometry with ignition and data collection devices, door open. (b) Oxygen mass fraction slice (blue to red, 0.04 to 0.23 kg/kg) for representative run showing the incursion of gravity current into the compartment.

evaluate grid sensitivity. Both the compartment and sand gas burner within were modeled, with the compartment floor at 1 m from the domain floor to mimic the experimental setup. The compartment is defined by adiabatic surfaces, and calculations were done from the door opened condition for 15 s, time sufficient to completely capture the backdraft phenomenon in this problem. Calculations took several minutes to a few days in local clusters at NIST.

As described in the previous section, 10 initial conditions were provided for species volume fractions and temperature in two zones within the compartment separated at a height from the compartment floor of 39.25 cm. Together with the option to define a low or mid-ignition location, 20 different simulations could be performed per grid resolution. Ambient initial conditions were specified outside of the compartment. A representative slice of oxygen concentration showing the incursion of the gravity current into the back of the compartment can be seen in figure 2b. In this figure, the dot on top of the gravity current front represents the ignition point for the low ignitor configuration. To model the ignition procedure consistently with the re-ignition model, a spark was defined in the corresponding ignitor location (low or mid spark) by placing a SPARK device. The ignition temperature threshold T_{TH} was therefore set to 0 K in the cell containing the device.

4. Grid sensitivity and comparisons with experiments

In Table 2, computed average gravity current height at the door H_{avg} and velocity U_{avg} , as well as total heat release, THR , are given as a function of grid size for two representative backdraft cases. These cases are methane, 25 kW, FFT = 450 s, and propane, 25 kW, FFT = 285 s. The fuel

Case [Fuel, Fire Size, FFT]	Grid	Δx (cm)	H_{avg} (cm)	U_{avg} (m/s)	THR (kJ)
Methane, 25 kW, 450 s	coarse	5.7	43.34	0.38	2693
Methane, 25 kW, 450 s	medium	2.8	44.61	0.49	2665
Methane, 25 kW, 450 s	fine	1.4	44.79	0.47	3580
Methane, 25 kW, 450 s	very fine	0.7	44.51	0.47	3619
Propane, 25 kW, 285 s	coarse	5.7	43.61	0.39	2357
Propane, 25 kW, 285 s	medium	2.8	44.41	0.51	2534
Propane, 25 kW, 285 s	fine	1.4	44.41	0.50	2716
Propane, 25 kW, 285 s	very fine	0.7	44.93	0.55	2780

Table 2: Grid sensitivity of two representative backdraft cases using methane and propane as fuels and low ignitor. Cases run in FDS LES mode, EXTINCTION_2 extinction model and $T_{TH} = 300^\circ\text{C}$.

219 load inside the compartment for these was such that a high probability of backdraft was seen in
 220 experiments. Both cases exhibited backdraft in calculations. The average gravity current height at
 221 the door was computed from the average zero of the normal velocity in the door symmetry plane
 222 between 0.5 s and 2 s (about the ignition time). Noise was noted on this function given by the
 223 vortical structures formed in the shear layer between hot and cold air regions, and this was more
 224 pronounced in finer grids, as expected. U_{avg} was computed by dividing the distance from the door
 225 to the ignition source by the time taken from door opening to ignition. In the simulations, the
 226 ignition time was computed as the time taken for the heat release rate HRR to increase over
 227 0.5kW. In FDS, THR is calculated by integrating equation (4) in the spatial domain and
 228 simulation time interval. It is seen that these global measures of the fluid evolution and backdraft
 229 event tend to converge for these benchmark cases as the grid is refined. Differences in H_{avg} are
 230 less than 2% among fine and very fine grids. Similarly, backdraft measures U_{avg} and THR show
 231 differences within 10%.

232 For reference, the total heat release measured in experiments for the methane, 25 kW, FFT = 450s
 233 case was $3470 \text{ kJ} \pm 520 \text{ kJ}$, and for the propane, 25 kW, FFT = 285 s case, was $2886 \text{ kJ} \pm 370 \text{ kJ}$.
 234 The dominating factor in the total heat release uncertainty attributes to the Type A evaluation of
 235 uncertainty, specifically the variance between repeated runs. The average total heat release
 236 measurements differ by about 30% and 6% with respect to the corresponding coarse and fine grid
 237 calculations. We note that fine grid calculations are within the uncertainty computed for these
 238 experimental ensemble averages. Also, the average gravity current height at the door estimated
 239 from video analysis of the Propane, 25 kW, FFT = 285 s case is 44.7 cm, differing about 2.5 %
 240 and 1 % with respect to coarse and fine grid estimates. Experimental U_{obs} computed from video
 241 analysis of time for ignition is 0.7 m/s and 0.5 m/s, respectively, in agreement with fine grid
 242 computation results (0.47 m/s and 0.50 m/s) and analytical estimations [?]. Gravity current
 243 estimated velocity values U_{est} are 0.48 m/s for the methane, 25 kW, FFT = 450 s case, and
 244 0.50 m/s for the propane, 25 kW, FFT = 285 s case.

245 Experiment pictures and simulation renders of the fireball exit for the Propane, 25 kW,

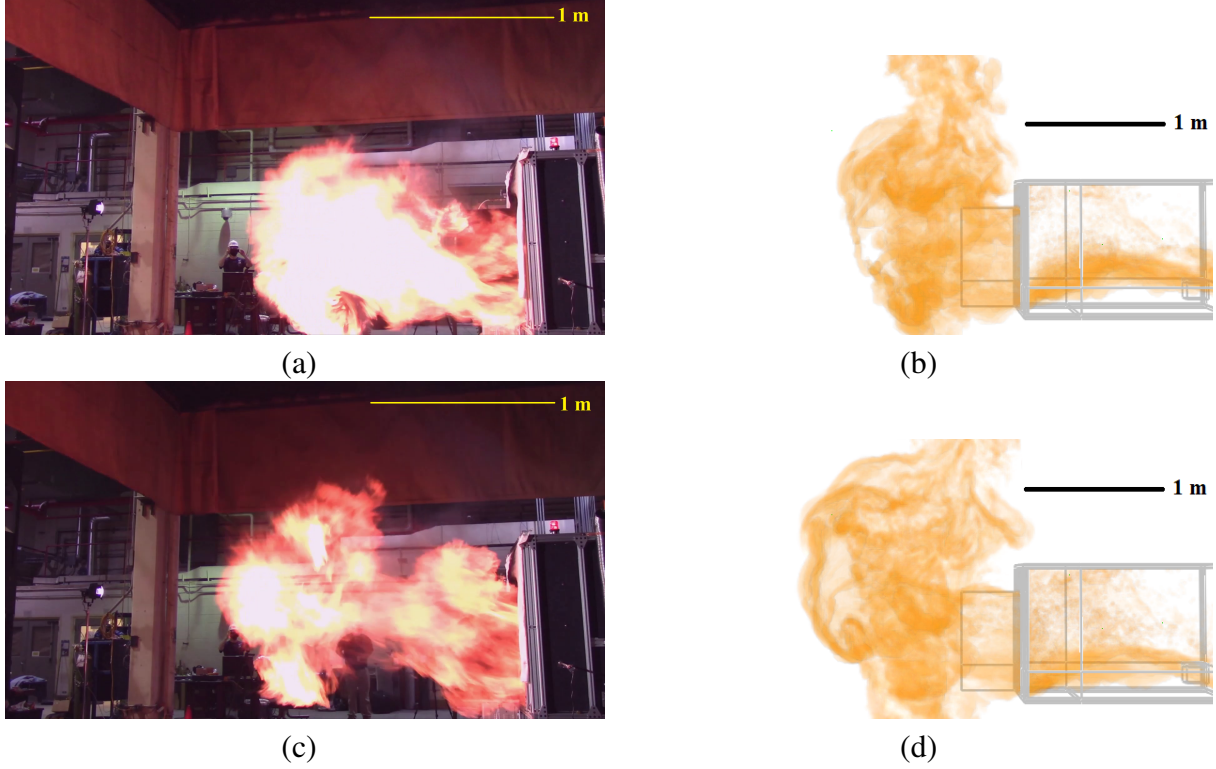


Figure 3. Backdraft exit deflagration from the door for propane, 25 kW, FFT = 285s case. (a) Experiment photograph at $t = 2.73$ from the door opening, (b) Smokeview HRRPUV render for fine grid simulation $t = 4.22$ s, (c) Experiment $t = 2.90$, and (d) Simulation $t = 4.37$ s.

FFT = 285s case are shown in Figure 3. In the simulation, Smokeview rendered pixels are colored where the heat release rate per unit volume is greater than 200 kW.m^{-3} and the temperature is higher than 600°C . Experiment and simulation quantities are not the same in this figure, but they provide insight into how the deflagration behaves in both cases. It is seen that the horizontal ejection of the deflagration is slightly weaker in the simulation, consistent with a slower evolution within the compartment. The time taken from door opening to fireball exit was estimated to be $2.66 \text{ s} \pm 0.7$, whereas this quantity in the fine grid simulation was 3.9 s. This result was seen using both extinction models, albeit less pronounced for EXTINCTION_1 (3.1 s), and also in methane simulations. The burning region close to the compartment's floor, as seen in calculations of Figure 3, is consistent with higher density and concentration of propane at door opening time. Most importantly, in the calculations of Table 2, the ignition threshold T_{TH} was set to 300°C . As shown in the next section, the number assigned to this parameter is critically important to obtain deflagration on numerical simulations of backdraft with fast mixing-controlled chemical reactions.

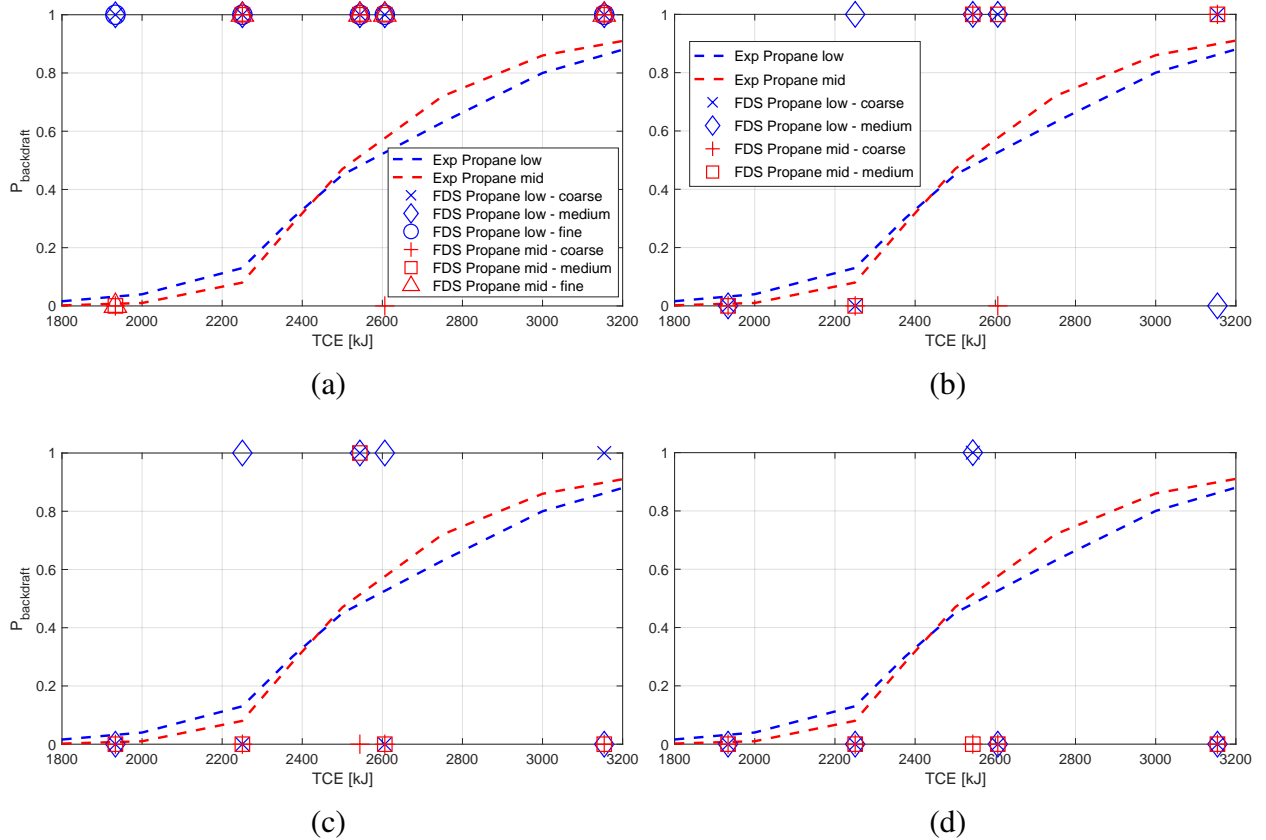


Figure 4. Simulated Backdraft events as a function of total fuel chemical energy TCE for propane. (a) Ignition model $T_{TH} = 300^{\circ}\text{C}$, (b) $T_{TH} = 325^{\circ}\text{C}$, (c) $T_{TH} = 350^{\circ}\text{C}$, and (d) $T_{TH} = 400^{\circ}\text{C}$.

260 5. Effect of ignition threshold

261 The re-ignition model T_{TH} primarily affects backdraft simulations with fast chemistry. To get an
 262 estimate for defining if the backdraft event happened in simulations, a test was devised comparing
 263 the total heat release THR and total heat release outside of the compartment THR_{EXT} with
 264 respect to the initial total chemical energy, TCE , of the fuel within the compartment. This last
 265 value is computed as $TCE = M_F \Delta H_F^o$, where M_F is the initial mass of fuel in the compartment,
 266 and ΔH_F^o is the fuel's heat of combustion obtained from Ref. [?]. Therefore, TCE is the
 267 maximum amount of thermal energy that can be produced by combustion. Backdraft is assumed
 268 to have happened if $THR > C_1 TCE$ and $THR_{EXT} > C_2 THR$. The constants C_1 and C_2 were
 269 set to 0.3, a value found to be sufficient to determine the deflagrations seen in the simulations.
 270 It was noted initially that using the default fuel auto-ignition temperature for T_{TH} would lead to
 271 having no deflagration for any of the 20 initial condition sets, irrespective of the grid refinement
 272 used. AITs in FDS are taken from reference [?] and are for methane and propane 540°C and
 273 450°C , respectively. In Figure 4, plots of backdraft events as a function of TCE for propane and

274 different values of $T_{TH} = 300, 325, 350, 400^\circ\text{C}$ are shown, for both "low" and "mid" ignitor
 275 positions. Superimposed are the backdraft probability, $P_{Backdraft}$, curves computed from the
 276 experiment, also as a function of the compartment fuel chemical energy load. It is emphasized
 277 that the results of simulations are *deterministic*. Therefore, in order to visualize their progression,
 278 "backdraft happened" in the simulations is assigned a value $P_{Backdraft} = 1$ in these plots, and
 279 "backdraft didn't happen" is given a $P_{Backdraft} = 0$. In Figure 4a, $T_{TH} = 300^\circ\text{C}$, fine grid results
 280 are also shown. Generally, the outcomes were not different between medium and fine refinement
 281 grids.

282 It is also observed that the backdraft outcomes are highly dependent on the temperature threshold
 283 of the FDS default re-ignition model. Within a small range of 100°C , outcomes range from
 284 "deflagration happened" being strongly over-predicted, to practically "no deflagration" simulated.
 285 This result is independent of the fuel load in the compartment. A value of $T_{TH} = 325^\circ\text{C}$ gives the
 286 best approximation to experiment-derived backdraft probability curves. Ideally, a good
 287 representative value of T_{TH} could be found, although it is unclear how that would have to be
 288 modified in different scenarios and for other fuels. This poses a great challenge for simulating
 289 these transient events using fast chemistry. We also note that analogous behavior was seen using
 290 the temperature controlled EXTINCTION_1 method. Similar trends were seen for methane, albeit
 291 transition was found to happen at a slightly lower temperature threshold for the ignition model,
 292 and more event variability with TCE was seen.

293 6. Effect of ignition procedure

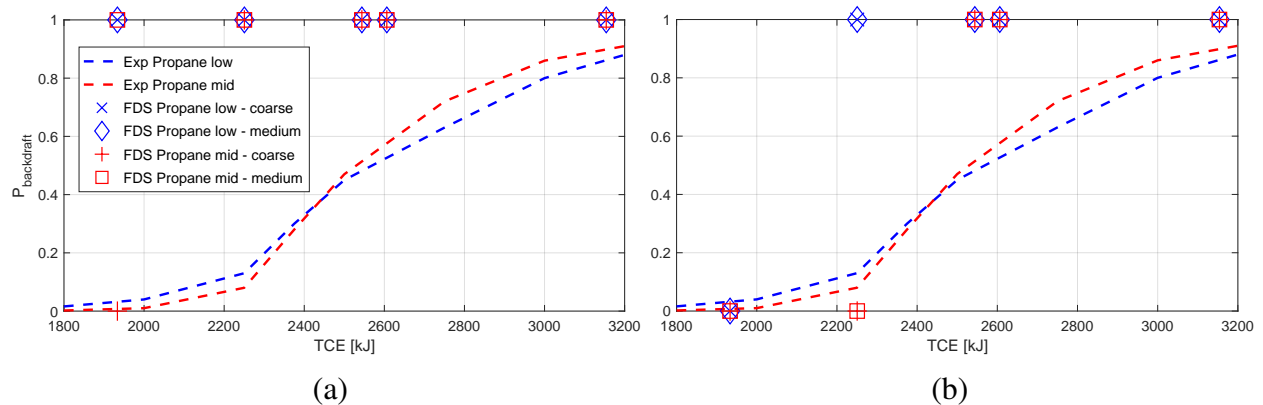


Figure 5. Simulated Backdraft events as a function of total fuel chemical energy TCE for propane and 8 spark grid ignitor. (a) Ignition model $T_{TH} = 300^\circ\text{C}$, (b) $T_{TH} = 350^\circ\text{C}$.

294 To test the effect of the ignition procedure in backdraft outcomes, a grid of 8 SPARK devices was
 295 defined in a horizontal plane area of 2 cm by 6 cm located near the experiments' ignition spark
 296 location. This resulted in a larger mesh volume that would undergo combustion in the ignitor
 297 region for each grid resolution, as the corresponding computational cells were assigned

298 $T_{TH} = 0$ K. For comparison, in Figure 5, similar plots to Figure 4 are shown for this larger spark
299 ignitor.

300 In terms of backdraft events, the effect of having a larger ignition volume is akin to using a
301 slightly lower T_{TH} in this problem. A larger ignitor volume where air and fuel can mix and react
302 potentially produces higher heat release and temperatures in computational cells surrounding the
303 ignition region. This leads to a larger chance of prompting deflagration. Similar issues have been
304 found when modeling piloted ignition of burners as observed in Ref. [?]. Although this behavior
305 is expected, it also points to the difficulty of modeling the complex thermo-chemical process of
306 fuel ignition by a spark when using simplified mixing-controlled combustion.

307 7. Conclusions

308 In this work, a wealth of experimental data was leveraged to define initial conditions and
309 validation information, which can be used to assess the capability of fire models in simulating
310 backdraft phenomena. Initial condition text data can be obtained by contacting the authors. A
311 model for said experiments was developed within the FDS framework and used to test the
312 simulation software with standard mixing-controlled fast chemical reactions.

313 Comparison with experiments of global backdraft quantities showed good agreement in relatively
314 fine grids and select high fuel load cases. Nevertheless, it was seen that backdraft simulation
315 presents a great challenge for fast chemistry combustion models used in realistic engineering
316 applications. In particular, simple ignition models based on a temperature threshold require
317 tuning this parameter. It was noted that variations of 50°C on this parameter could significantly
318 change backdraft outcomes across various grids, ignition sources, and initial conditions. Ideally, a
319 variation of the re-ignition model that is not as sensitive to a hand-picked temperature parameter
320 would be available. An option being considered by this group is the use of a test temperature that
321 is not only the mean cell temperature but also contains a subgrid component.

322 On the other hand, it was shown that the ignition procedure based on dropping the temperature
323 threshold at the ignition source location also greatly influences the backdraft simulation outcome.
324 It is unclear how the ignition volume should be defined for backdraft triggered by point sources
325 like sparks, and more study is required on this topic. Further, in these calculations uniform
326 composition and temperature conditions in two zones were used from experiment sensor averages.
327 The effect of this simplification in the results should be tested. One possible way is to actually
328 simulate the fuel loading process in the compartment up to door opening. Another option is to add
329 stochastic disturbances of initial composition fields to assess their effect in backdraft outcomes.

330 Finally, the experiments modeled in this work involved simple hydrocarbon gases, with known
331 chemical and thermal properties. In real fires, gaseous fuels are the product of complex pyrolysis
332 processes and therefore backdraft outcomes are expected to be heavily influenced by their
333 combustion characteristics. Although not touched upon, experiments similar to the ones described
334 in section 2 were also performed using wood-cribs as fuel. Their modeling and analysis is left for a
335 future effort.

336 **References**

- 337 [1] C. M. Fleischmann, Z. Chen, Defining the difference between backdraft and smoke
338 explosions, Procedia Engineering 62 (2013) 324–330.
- 339 [2] C. Fleischmann, *Backdraft phenomena*, Ph.D. thesis, University of California, Berkeley,
340 Berkeley, USA (1993).
- 341 [3] C. Fleischmann, P. Pagni, R. Williamson, Quantitative backdraft experiments, in: Fire
342 Safety Science-Proceedings of the Fourth International Symposium, 1994, pp. 337–348.
- 343 [4] D. Gottuk, M. Peatross, J. Farley, F. Williams, The development and mitigation of backdraft:
344 a real-scale shipboard study, Fire Safety Journal 33 (4) (1999) 261–282.
- 345 [5] J. Wu, Y. Zhang, X. Gou, M. Yan, E. Wang, L. Liu, Experimental research on gas fire
346 backdraft phenomenon, Procedia Environmental Sciences 11 (2011) 1542–1549.
- 347 [6] H. Hayasaka, Y. Kudo, H. Kojima, T. Hashigami, J. Ito, T. Ueda, Backdraft experiments in a
348 small compartment, in: Progress in Scale Modeling: Summary of the First International
349 Symposium on Scale Modeling (ISSM I in 1988) and Selected Papers from Subsequent
350 Symposia (ISSM II in 1997 through ISSM V in 2006), Springer, 2008, pp. 313–324.
- 351 [7] L. Tsai, C. Chiu, Full-scale experimental studies for backdraft using solid materials, Process
352 Safety and Environmental Protection 91 (3) (2013) 202–212.
- 353 [8] J. Zhao, Y. Li, J. Li, Y. Huang, J. Wu, Experimental study on the backdraft phenomenon of
354 solid fuel, Plos one 16 (8) (2021) e0255572.
- 355 [9] W. Weng, W. Fan, Y. Hasemi, Prediction of the formation of backdraft in a compartment
356 based on large eddy simulation, Engineering Computations 22 (4) (2005) 376–392.
- 357 [10] S. Ferraris, J. Wen, S. Dembele, Large eddy simulation of the backdraft phenomenon, Fire
358 Safety Journal 43 (3) (2008) 205–225.
- 359 [11] J. Park, C. Oh, Y. Han, K. Do, Computational study of backdraft dynamics and the effects of
360 initial conditions in a compartment, Journal of Mechanical Science and Technology 31 (2)
361 (2017) 985–993.
- 362 [12] S. G. Ashok, T. Echekki, A numerical study of backdraft phenomena under normal and
363 reduced gravity, Fire Safety Journal 121 (2021) 103270.
- 364 [13] D. Myilsamy, C. B. Oh, B.-I. Choi, Large eddy simulation of the backdraft dynamics in
365 compartments with different opening geometries, Journal of Mechanical Science and
366 Technology 33 (2019) 2189–2201.
- 367 [14] R. Falkenstein-Smith, T. Cleary, Thermal and gas mixture composition measurements
368 preceding backdrafts in a 2/5th scale compartment, NIST Technical Note 2185, National
369 Institute of Standards and Technology (2022).

- 370 [15] V. Babrauskas, W. Parker, G. Mulholland, W. Twilley, The phi meter: A simple,
371 fuel-independent instrument for monitoring combustion equivalence ratio, Review of
372 Scientific Instruments 65 (7) (1994) 2367–2375.
- 373 [16] R. Falkenstein-Smith, T. Cleary, The Design and Performance of a Second-Generation Phi
374 Meter, NIST Technical Note 2184, National Institute of Standards and Technology (2021).
- 375 [17] C. Brown, R. Falkenstein-Smith, T. Cleary, Reduced-Scale Compartment Gaseous Fuels
376 Backdraft Experiments, NIST Technical Note 2183, National Institute of Standards and
377 Technology (2021).
- 378 [18] M. Hurley (Ed.), SFPE Handbook of Fire Protection Engineering, 5th Edition, Springer,
379 New York, 2016.
- 380 [19] B. Magnussen, B. Hjertager, On Mathematical Modeling of Turbulent Combustion with
381 Special Emphasis on Soot Formation and Combustion, in: Proceedings of the Sixteenth
382 Symposium (International) on Combustion, Combustion Institute, Pittsburgh, Pennsylvania,
383 1977, pp. 719–729.
- 384 [20] K. McGrattan, S. Hostikka, R. McDermott, J. Floyd, C. Weinschenk, K. Overholt, Fire
385 Dynamics Simulator, Technical Reference Guide, National Institute of Standards and
386 Technology, Gaithersburg, Maryland, USA, and VTT Technical Research Centre of Finland,
387 Espoo, Finland, sixth Edition, vol. 1: Mathematical Model; Vol. 2: Verification Guide;
388 Vol. 3: Validation Guide; Vol. 4: Software Quality Assurance (September 2013).
- 389 [21] C. Beyler, SFPE Handbook of Fire Protection Engineering, 5th Edition, Springer, New York,
390 2016, Ch. Flammability Limits of Premixed and Diffusion Flames.
- 391 [22] W. Pitts, The Global Equivalence Ratio Concept and the Formation Mechanisms of Carbon
392 Monoxide in Enclosure Fires, Progress in Energy and Combustion Science 21 (1995)
393 197–237.
- 394 [23] M. Bundy, A. Hamins, E. Johnsson, S. Kim, G. Ko, D. Lenhert, Measurements of Heat and
395 Combustion Products in Reduced-Scale Ventilation-Limited Compartment Fires, NIST
396 Technical Note 1483, National Institute of Standards and Technology, Gaithersburg,
397 Maryland (2007).
- 398 [24] G. Forney, Smokeview, A Tool for Visualizing Fire Dynamics Simulation Data, Volume I:
399 User's Guide, National Institute of Standards and Technology, Gaithersburg, Maryland,
400 USA, sixth Edition (May 2013).
- 401 [25] K. McGrattan, S. Hostikka, R. McDermott, J. Floyd, C. Weinschenk, K. Overholt, Fire
402 Dynamics Simulator, User's Guide, National Institute of Standards and Technology,
403 Gaithersburg, Maryland, USA, and VTT Technical Research Centre of Finland, Espoo,
404 Finland, sixth Edition (September 2013).

- 405 [26] M. Khan, A. Tewarson, M. Chaos, SFPE Handbook of Fire Protection Engineering, 5th
406 Edition, Springer, New York, 2016, Ch. Combustion Characteristics of Materials and
407 Generation of Fire Products.
- 408 [27] J. P. White, S. Vilfayeau, A. W. Marshall, A. C. Trouv , R. J. McDermott, Modeling flame
409 extinction and reignition in large eddy simulations with fast chemistry, *Fire Safety Journal*
410 90 (2017) 72–85.

411 **Figure captions**

- 412 Figure 1. Schematic of the 2/5th scale compartment used in backdraft experiments
- 413 Figure 2. Backdraft computational model : (a) Domain and compartment geometry with ignition
414 and data collection devices, door open. (b) Oxygen mass fraction slice (blue to red, 0.04 to 0.23
415 kg/kg) for representative run showing the incursion of gravity current into the compartment.
- 416 Figure 3. Backdraft exit deflagration from the door for propane, 25 kW, FFT = 285s case. (a)
417 Experiment photograph at $t = 2.73$ s from the door opening, (b) Smokeview HRRPUV render for
418 fine grid simulation $t = 4.22$ s, (c) Experiment $t = 2.90$, and (d) Simulation $t = 4.37$ s.
- 419 Figure 4. Simulated Backdraft events as a function of total fuel chemical energy TCE for
420 propane. (a) Ignition model $T_{TH} = 300^\circ\text{C}$, (b) $T_{TH} = 325^\circ\text{C}$, (c) $T_{TH} = 350^\circ\text{C}$, and (d)
421 $T_{TH} = 400^\circ\text{C}$.
- 422 Figure 5. Simulated Backdraft events as a function of total fuel chemical energy TCE for
423 propane and 8 spark grid ignitor. (a) Ignition model $T_{TH} = 300^\circ\text{C}$, (b) $T_{TH} = 350^\circ\text{C}$.